



HAL
open science

Parameter estimation of gaussian heat flux : investigation of stationnary Gas Tungsten Arc Welding (GTAW) operation

Sébastien Rouquette

► **To cite this version:**

Sébastien Rouquette. Parameter estimation of gaussian heat flux : investigation of stationnary Gas Tungsten Arc Welding (GTAW) operation. Quatrièmes Journées des Démonstrateurs en Automatique, Jun 2013, Angers, France. hal-01777999

HAL Id: hal-01777999

<https://hal.science/hal-01777999>

Submitted on 25 Apr 2018

HAL is a multi-disciplinary open access archive for the deposit and dissemination of scientific research documents, whether they are published or not. The documents may come from teaching and research institutions in France or abroad, or from public or private research centers.

L'archive ouverte pluridisciplinaire **HAL**, est destinée au dépôt et à la diffusion de documents scientifiques de niveau recherche, publiés ou non, émanant des établissements d'enseignement et de recherche français ou étrangers, des laboratoires publics ou privés.

Parameter estimation of gaussian heat flux: investigation of stationary Gas Tungsten Arc Welding (GTAW) operation.

Sebastien Rouquette^{1,2}

¹ Laboratoire de Mécanique et Génie Civil UMR 5508, Université de Montpellier 2, 34095 Montpellier, France.

² Department of Materials Sciences and Metallurgy, University of Cambridge, Pembroke street, CB2 3QZ, Cambridge, United Kingdom. Tel: +44(0)122333 1950

sebastien.rouquette@univ-montp2.fr

A mathematical modelling has been established in order to predict the weld pool shape evolution in the frame of stationary gas tungsten arc welding experiment. In this mathematical modelling, the heat flux was modelled with a Gaussian function. This heat flux represents the energy generated by the electrical arc and absorbed into the work-piece. An inverse approach is used for estimating the parameters describing this heat flux from the “measured” temperatures. The Gradient Conjugate Method is used for solving the inverse problem. An adjoint problem is also solved in order to compute the gradient of the objective function. The aim of this communication is to check numerically the feasibility of the inverse problem and its robustness to random measurement errors.

Keywords: gradient conjugate, adjoint problem, inverse heat transfer problem.

1. Introduction

Welding processes are widely employed in manufacturing industries such automobiles, airplanes, petrochemical plants or again nuclear power stations. These structures require high level of safety what means high quality of joint properties (mechanical and microstructure). Few manufacturing welding processes reach such level of performance when its control is well handled. Gas tungsten arc welding (GTAW) is one of the most widely employed welding processes that is applied with success for welding of stainless steels and non-ferrous materials. In this process, a tungsten electrode is shielded with a flow of either pure inert gas such as argon or helium or a mixture of both gases (some nitrogen or hydrogen can be added). The assembly of work pieces is obtained through a local fusion due to the heat generated from an electrical arc.

The analysis of the physical phenomenon (electromagnetism, fluid flow, heat transfer ...) that takes place in the process is crucial to understand, for example, weld pool formation [1, 2] as well as microstructure changes in the thermally affected base metal [3] and residual stress distribution in the joint [4]. The heat flux absorbed within the work piece must be known accurately in order to better understand all the mechanical and metallurgical consequences of the welding operation.

In order to perform a reliable multi-physics simulation of the work piece, it is extremely important to know correctly the heat input absorbed into the work piece. Inverse heat conduction problem represents an alternative approach of obtaining the heat flux incoming into the work piece. This present work is also a preliminary study on the heat flux estimation of gta welding spot. The main goal of this work is to validate numerically the estimation of the unknown parameters (gtaw efficiency and heat flux distribution) with temperature measurements.

2. GTAW multiphysic problem

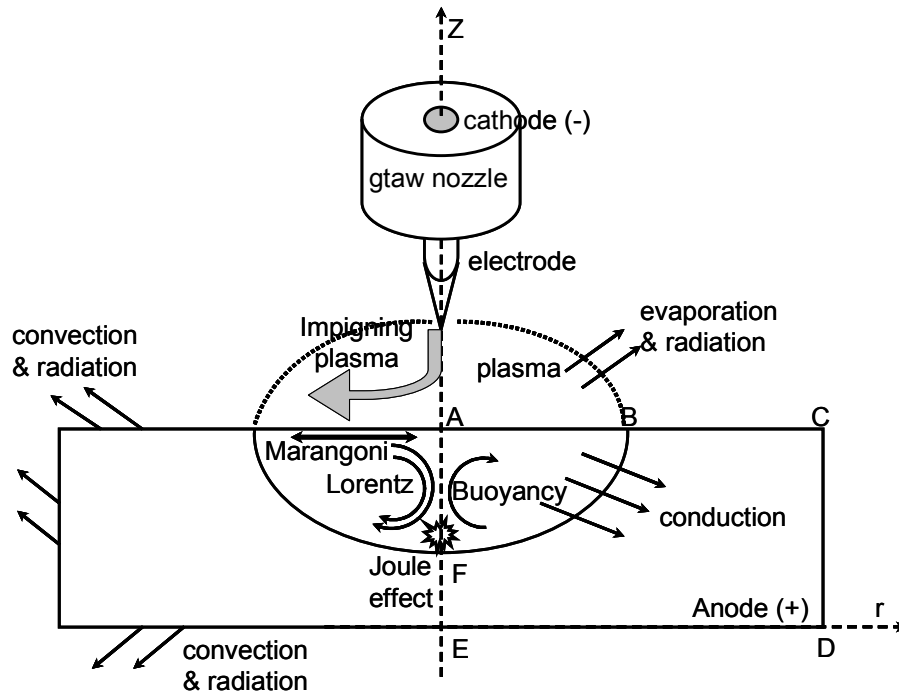


Figure 1: physical phenomena involved in gta welding [5].

Gtaw operation involves several phenomena: heat transfer, electromagnetism, fluid flow, phase transformation, free surface, deformation ... these overall phenomena are represented in figure 1. The weld pool (molten metal) is driven through a combination of forces: Buoyancy (Boussinesq), Lorentz (electromagnetic), Marangoni (surface tension) and Impinging plasma. The fusion of the metallic work piece is due to the high thermal energy generated by the electrical arc between the electrode tip and work piece surface. There is also some volumetric heat generated within the work piece due to the electric current also called Joule effect.

2.1 GTAW assumptions

The following assumptions are made in order to simplify the gtaw model:

- The study is restricted to stationary spot welding so the problem is axisymmetric.
 - The flow is laminar and incompressible due to the small size of the weld pool.
 - The thermo-physical properties of the 304L stainless steel are temperature dependent as well as the surface tension coefficient.
 - The magnetic field is not considered as the Lorentz force is known to be a minor one for intensities below 200A [1]
 - The cylindrical work piece is immobile and it is kept up with four rods in order to limit any heat transfer by conduction. The radius and thickness are respectively 40mm and 4mm .
 - The arc plasma is not modelled as well as the free surface of the weld pool.
- Based on these above assumptions, the governing partial differential equations are expressed in the (r, z) coordinate system.

2.2 Comparison of numerical results with experimental data

The reader will find the details of the governing equations (heat transfer and fluid flow) in [7] as well as the values of the constant used in the simulation except for the thermal conductivity, specific heat, mass density and dynamic viscosity are chosen as temperature dependent and their evolution are taken from [6].

The finite element software used for this simulation is Elmer (<http://www.csc.fi/english/pages/elmer>). Elmer is a finish Open Source Finite Element Software for Multiphysical Problems developed by the CSC – IT Center for Science. The mesh was realised with Gmsh software (<http://geuz.org/gmsh/>). The mesh consisted of 840 nodes and 1564 triangle finite elements. The order of the finite element was set to 1 for the temperature and the fluid velocity and 0 for the pressure.

Table 1: GTAW experimental conditions

\tilde{I}_w	150A	\tilde{U}_w	10.4V
Shielding gas	argon	Arc length	2mm
Disc thickness	6mm	Disc radius	50mm
Electrode type	tungsten	Electrode diameter	2.4mm

The experimental conditions for the stationary gtaw are summarized in table 1. The average welding intensity and tension are respectively 150A and 10.4V. The values used in the simulation are the ones measured on the welding generator. Welding intensity and tension are simultaneously measured with temperature measurements as well as the top surface evolution of the weld pool is recorded with a high speed camera. These data are reported in figure 2 and 3.

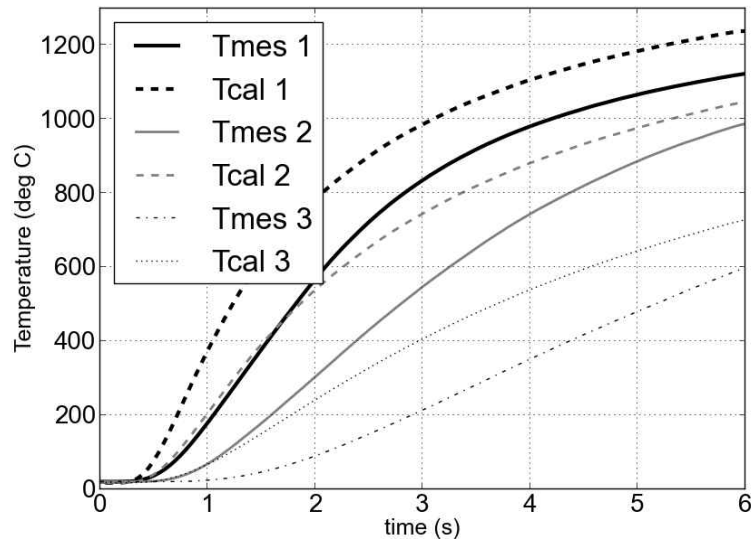


Figure 2: comparison between measured and simulated temperatures.

The temperatures were measured at three different positions on the backside of the stainless steel disc. The positions were respectively: 0mm (Tmes 1), 4mm (Tmes 2) and 8mm (Tmes 3). The maximum temperature of the disc back side is about 1100°C for sensor 1, see figure 3. On the backside of the disc, it can be evaluated that the thermal gradient is about 62.5°C/mm while it was about 150°C/mm on the symmetry axis (the weld pool width was estimated to 1.5mm from a macrograph not presented here). These thermal gradients are quite classic during welding operations. The final radius of the weld pool was about 5.5 mm for a 5.8s arc duration.

The established gtaw model overestimates the measured temperatures at the three sensors, see figure 2, as well as it underestimate the weld pool radius, figure 3.

The comparison between experimental and calculated temperatures and weld pool radius shows some important discrepancies. In this simulation gtaw efficiency and gaussian radius were evaluated from the literature and they are constant parameters. These two parameters must be known accurately as they influence the heat flux distribution. Then, it is proposed to estimate these parameters with an inverse heat transfer technique in the next chapter. In addition, the gtaw efficiency is supposed to vary with the time in order to capture some transient phenomena between the arc plasma and the steel disc.

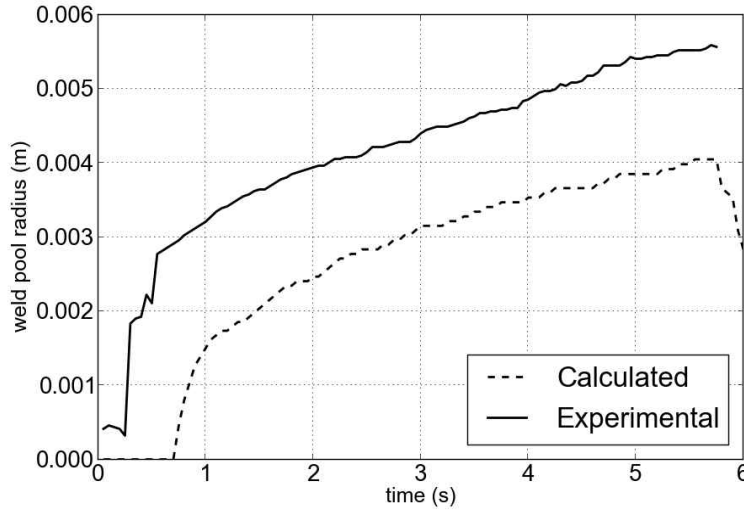


Figure 3: comparison between measured and simulated weld pool radii.

3. Inverse heat transfer problem (ihtp)

In order to simplify the stated direct problem in the previous chapter, this chapter will deal with an inverse heat conduction problem only. Once the basis of this simplified inverse problem is made, it will be extended to the thermo-convective gtaw case. The aim of this inverse problem is to estimate a time varying gtaw efficiency and a constant gaussian radius parameter.

Energy conservation with no convective transport:

$$\rho C_p^{eq} \frac{\partial T}{\partial t} - \frac{1}{r} \frac{\partial}{\partial r} \left(r \lambda \frac{\partial T}{\partial r} \right) - \frac{\partial}{\partial z} \left(\lambda \frac{\partial T}{\partial z} \right) = 0 \text{ in } \Omega \times I \quad (1)$$

with $C_p^{eq} = C_p + \Delta H_f \frac{f_L}{T}$ and f_L is the liquid fraction:

$$f_L = \begin{cases} 1 & \text{if } T > T_L; \\ \frac{T - T_S}{T_L - T_S} & \text{if } T_S \leq T \leq T_L; \\ 0 & \text{if } T < T_S \end{cases} \quad (2)$$

With the following boundary conditions are:

$$-\lambda \frac{\partial T}{\partial z} = -\Phi(r, t) = \eta \frac{1}{2} \frac{U_w(t) I_w(t)}{\pi R_b^2} e^{-\frac{1}{2} \left(\frac{r}{R_b} \right)^2} \quad \text{on } \Gamma_{AB} \times I \quad (3)$$

$$-\lambda \frac{\partial T}{\partial n} = h(T - T_0) + \varepsilon \sigma (T^4 - T_0^4) \quad \text{on } \Gamma_{BC} \cup \Gamma_{CD} \cup \Gamma_{DE} \times I \quad (4)$$

$$-\lambda \frac{\partial T}{\partial r} = 0 \quad \text{on } \Gamma_{EF} \cup \Gamma_{FA} \times I \quad (5)$$

The initial condition is:

$$T(r, t = 0) = T_0 \quad \text{in } \Omega \quad (6)$$

$\Phi(r, t)$ is the heat flux exchanged between the argon arc plasma and the top surface work-piece. The heat flux distribution is modelled with a Gaussian distribution [7]. U_w and I_w are respectively the measured welding tension and intensity, $\eta(t)$ is the gtau efficiency and R_B is the Gaussian radius.

Inverse heat transfer problems are known to be ill posed [8] in contrast to the direct heat transfer problems which are well posed. In this latter, the solution exists, the solution is unique and the solution is stable to small changes in the input data.

A variety of numerical techniques have been proposed for the solution of inverse problems dealing with heat transfer problems. As examples, Murio [9] developed the mollification method, Alifanov [10] with co-workers suggested and developed the iterative regularization method. In this approach an optimization problem is solved, using a method such as the conjugate gradient, being the gradient equation determined by an adjoint problem [11]. This latter technique is used in this work for the estimation of the time varying gtau efficiency and its gaussian radius distribution.

3.1 Statement of the inverse heat transfer problem

The IHTP general formulation is written as [12]:

Find the vector \bar{p} which minimizes the cost function $S(\bar{p})$:

$$S(\bar{p}) = \frac{1}{2} \int_{t_0}^{t_f} \int_{\Omega} \sum_{i=1}^{n_s} (Y_{meas}(t) - T_{cal}(x_i, t; \bar{p}))^2 d\Omega dt$$

where Y_{meas} are the measured temperatures and T_i the calculated temperatures at point x_i , $i = 1, \dots, n_s$.

3.2 Gradient conjugate method with the adjoin and sensitivity problems

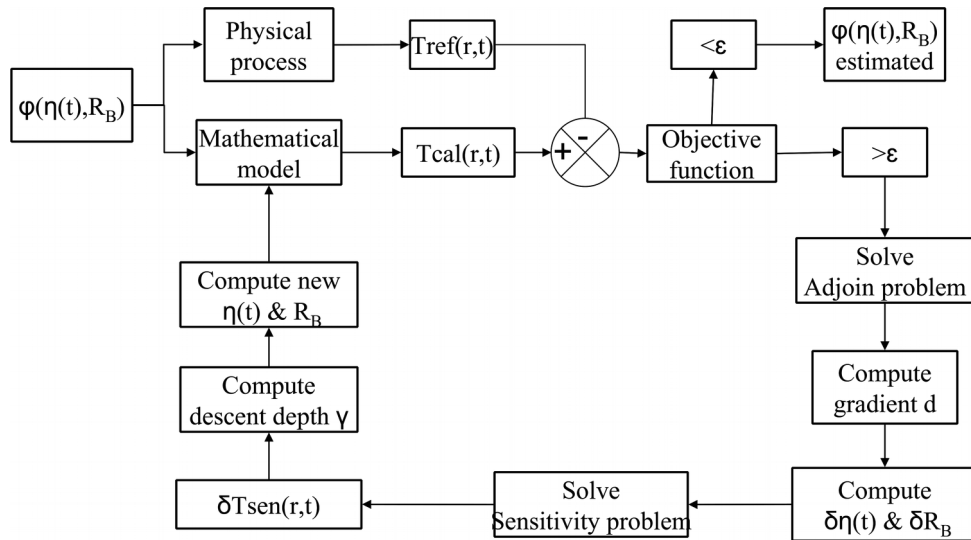


Figure 4: Gradient conjugate algorithm with adjoin problem.

The gradient conjugate algorithm is presented in figure 4. This method requires first to solve the mathematical model which describes the investigated process. Then, calculated temperatures are compared to measured temperatures on the real process. Then, the objective function as defined in (7) is computed. If the objective function is greater than a defined threshold, say 10^{-3} , the iterative process starts in order to estimate the unknown parameters. The unknown parameters are: a time dependent efficiency: $\eta(t)$ and the gaussian radius distribution: R_B . The iterative process consists in solving the adjoint problem in order to get the gradient of the objective function. Hence, the sensitivity problem is solved in the aim to compute the descent depth. Once, the gradient and the descent depth are computed, the new set of unknown parameters are evaluated. The mathematical problem is solved again with the updated unknown parameters until the objective function reaches the predefined threshold or a given number of iterations.

The adjoint and sensitivity problems are quickly defined in the paragraphs below. The reader can refer to [12] to understand the details of their computation. Then, the gradient expressions of the objective function are also given without any details. The reader can refer to [12] for the expression of the descent depth.

The adjoint problem:

The adjoint equations are obtained by solving the following minimization problem defined by the cost function under the constraint of the heat conduction equation:

$$L(T, p, \psi) = S(p) + \int_T \int_{\Omega} \left(\rho C_p \frac{\partial T}{\partial t} - \nabla(\lambda(\nabla T)) \right) \psi dt d\Omega \quad (8)$$

where a Lagrange function $\psi(r, t; z)$ is introduced. Adjoint equations are obtained when the following conditions is checked: $\frac{\partial L}{\partial \theta} \delta \theta = 0$ (for a fixed value $\psi(x, t; z)$). The adjoint equations are defined by the equations (9) to (12):

$$\rho C_p^{eq} \frac{\partial \psi}{\partial t} - \frac{1}{r} \frac{\partial}{\partial r} \left(r \lambda \frac{\partial \psi}{\partial r} \right) - \frac{\partial}{\partial z} \left(\lambda \frac{\partial \psi}{\partial z} \right) = E(r_i, t; p) \quad \text{in } \Omega \times I \quad (9)$$

With the following boundary conditions (16)-(17) and final condition (18):

$$-\lambda \frac{\partial \psi}{\partial n} = (h + 4\varepsilon\sigma T^3) \psi \quad \text{on } \Gamma_{AB} \cup \Gamma_{BC} \cup \Gamma_{CD} \cup \Gamma_{DE} \times I \quad (10)$$

$$-\lambda \frac{\partial \psi}{\partial r} = 0 \quad \text{on } \Gamma_{EF} \cup \Gamma_{FA} \times I \quad (11)$$

$$\psi(r, t = t_{end}) = 0 \quad \text{in } \Omega \quad (12)$$

Remark: $E(r_i, t; p) = \int_{\Omega} (T(r_i, t; p) - T_{meas}(t)) \delta(x - x_i) d\Omega$.

The sensitivity problem:

The sensitivity equations are defined as follows:

$$\delta T = \lim_{\alpha \rightarrow 0} \frac{T(r, t; p - \alpha \delta p) - T(r, t; p)}{\alpha} \quad (13)$$

Where δT is the sensitivity function which results of a small variation $\delta p = \{\delta \eta, \delta R_B\}$ of the unknown parameters of the heat flux. Applying (13) leads to the sensitivity equations (14) to (18):

$$\rho C_p^{eq} \frac{\partial \delta T}{\partial t} - \frac{1}{r} \frac{\partial}{\partial r} \left(r \frac{\partial \lambda \delta T}{\partial r} \right) - \frac{\partial}{\partial z} \left(\frac{\partial \lambda \delta T}{\partial z} \right) = 0 \quad \text{in } \Omega \times I \quad (14)$$

Associated to the following boundary conditions and initial condition:

$$-\lambda \frac{\partial \delta T}{\partial z} = -\frac{U_W I_W}{2\pi} \left\{ \frac{\delta \eta(t)}{R_B^2} - \frac{2\eta(t)\delta R_B}{R_B^3} \right\} \exp\left(-0.5\left(\frac{r}{R_B}\right)^2\right) \Gamma_{AB} \times I \quad (15)$$

$$-\lambda \frac{\partial \delta T}{\partial r} = (h + 4\varepsilon\sigma T^3) \delta T \quad \Gamma_{BC} \cup \Gamma_{CD} \cup \Gamma_{DE} \times I \quad (16)$$

$$-\lambda \frac{\partial \delta T}{\partial r} = 0 \quad \text{on } \Gamma_{EF} \cup \Gamma_{FA} \times I \quad (17)$$

$$\delta T(r, t = 0) = 0 \quad \text{in } \Omega \quad (18)$$

Gradient expressions:

The gradient of the objective function is deduced from the adjoin function $\psi(x, t; z)$ when:

$$dL = \frac{\partial L}{\partial p} \delta p = \langle \nabla S(T, p), \delta p \rangle \quad \text{with} \quad \nabla S(T, p) = \frac{\partial S(T, p)}{\partial p} \quad \text{and} \quad \frac{\partial L}{\partial T} \delta T = 0.$$

Consequently, the gradient of the objective function according to gtaw efficiency is:

$$\nabla S_\eta = \int_T \int_{\Gamma_{AB}} \frac{U_W I_W}{2\pi R_B^2} \cdot \exp\left(-0.5\left(\frac{r}{R_B}\right)^2\right) \psi(x, t; z) dt d\Gamma_{AB} \quad (19)$$

While the gradient with respect to gaussian radius R_B is:

$$\nabla S_{R_B} = -\int_T \int_{\Gamma_{AB}} \frac{U_W I_W \eta(t)}{\pi R_B^3} \cdot \exp\left(-0.5\left(\frac{r}{R_B}\right)^2\right) \psi(x, t; z) dt d\Gamma_{AB} \quad (20)$$

3.3 Numerical inverse analysis with exact data and noised data

Three cases are investigated here. The goals of this numerical work are double:

- First, we verify that the inverse heat transfer problem converges towards the exact parameters whatever is the initial set of parameters (cases “Exact 1” and “Exact 2”);
- Secondly, we want to evaluate the robustness of the inverse algorithm to some noise measurement on the temperature used. Then, a random error is added to the reference temperature with a maximum standard deviation $\sigma(t)$ of 5% of the current temperature (e.g. $|\sigma(t)| \leq 5\% \times T_{REF}(t)$ so it comes: $T_{NOISE}(t) = T_{REF}(t) + \sigma(t)$).

For this numerical study, reference temperatures are required for solving the ihtp. These reference temperatures have been obtained with a given values for the gtaw efficiency and gaussian radius. The time variation of gtaw efficiency is shown in figure 6 as the red curve. The gaussian radius R_B was set to 3.2 mm. The duration of the simulation was 5s. For the cases “Exact 1” and “Noised”, the parameters were initialized to 0.1 for the efficiency and 10mm for R_B . For case “Exact 2”, the parameters were initialized to 0.9 for the efficiency and 1mm for R_B .

Figure 5 presents the evolution of the three objective functions along the iterative process. The two objective functions for cases “exact 1 & 2” decreased monotonously to low values: 25.4 and 503.1 respectively. The “noised” case decreased for 20 iterations before stabilizing to an average value of 1.9e4. This behaviour is classically observed with data including noise measurement.

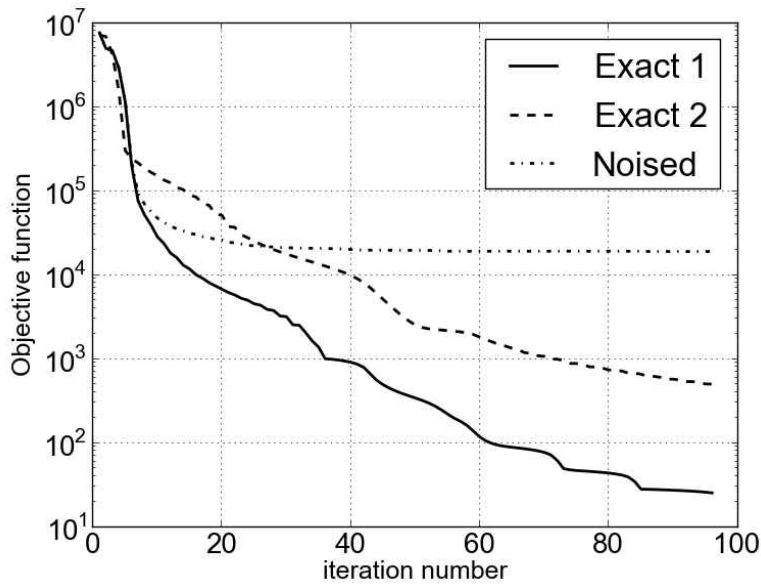


Figure 5: evolution of the objective function along the iteration process.

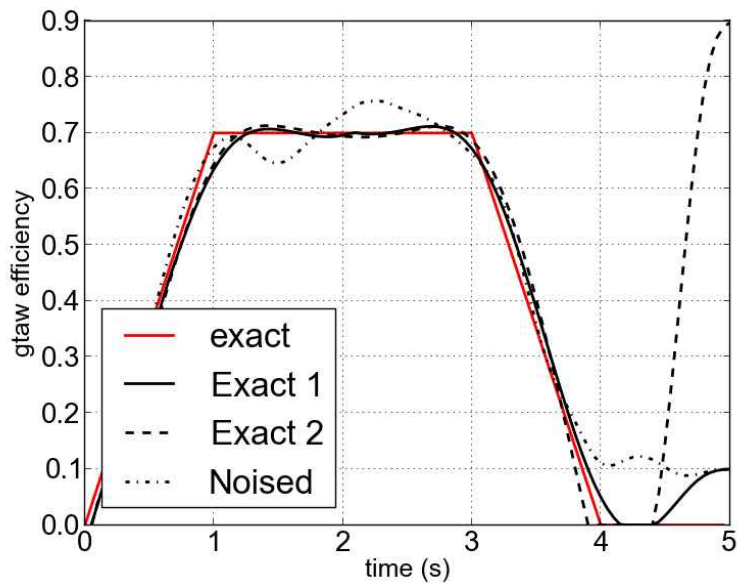


Figure 6: estimated efficiency along the iteration process.

Figures 6 and 7 present the estimated parameters at the final iteration of the ihtp (so the 95th iteration here). For the two exact cases, both the efficiency and gaussian radius are accurately estimated. It can be noticed that the efficiency value for the final time is incorrectly estimated due to the final condition of the adjoint problem, see equation (12). The efficiency value could have been imposed to zero at the final time as experimentally the arc will be switched off. With noise measurement, the efficiency is still estimated but some discrepancies are noticeable in comparison to the exact value. The estimated efficiency is still in good agreement with the exact one despite a noise measurement. The gaussian radius is very well estimated for the three investigated cases, figure 7. The noise measurement finally affected mostly the efficiency parameter. This due to the assumption done on the efficiency parameter: this parameter is defined for each step time of the simulation so for a simulation of 5s with a step time of 0.05s, it

consisted of 100 parameters to estimate for the efficiency. While the gaussian radius was defined with one parameter for all the simulation.

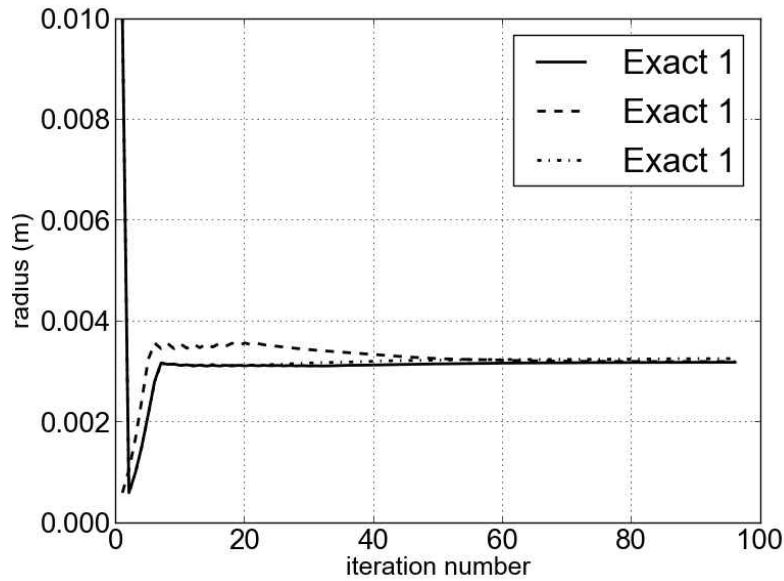


Figure 7: estimated gaussian radii along the iteration process.

The temperature residuals for the “noised” cases is proposed in figure 8. For the two other cases, this results are not relevant as this temperature difference was lower than 2°C. For the “noised” case, the temperature difference is large due to the noise added to the reference data. Despite, this important noise, the gradient conjugate method was robust and led to a good estimation of the efficiency and gaussian radius parameters.

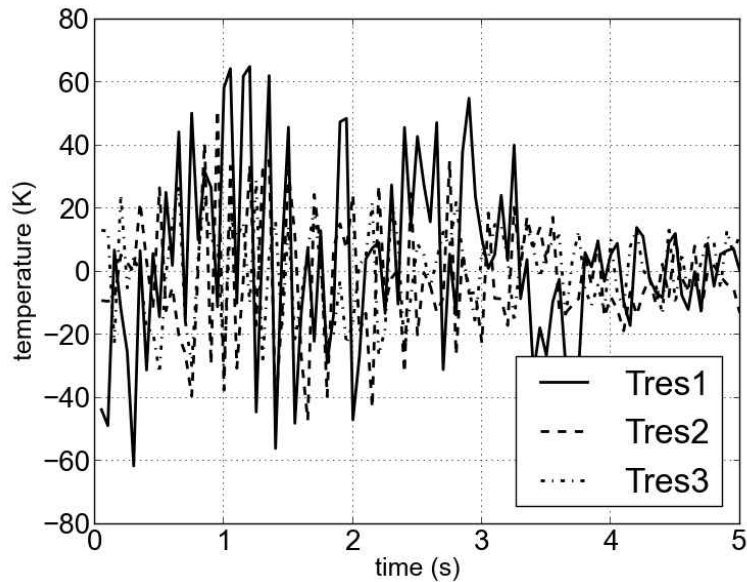


Figure 8: evolution of the temperature residual with respect to the time.

4 Conclusions

A gtaw modelling have been established in a previous work [19]. The comparison of the numerical results with the experimental data exhibited lots of discrepancies between the

calculated and measured temperatures on one hand and between the calculated and measured weld pool radius on the other hand. Assuming that the gtaw stated modelling was correct, it occurred that the heat flux exchanged between the arc plasma and the steel disc was not known correctly. The heat flux absorbed by the work piece is supposed to be Gaussian and defined with two main parameters: process efficiency and gaussian radius. An inverse heat transfer problem is developed in order to estimate these unknown parameters from “experimental” data. The optimization method used for solving the inverse problem is the gradient conjugate method.

The inverse heat transfer problem was investigated through few numerical cases in order to be sure that it gives the right data on one hand and it was robust to noise measurement on the other hand. The inverse problem gave successful results with the reference temperature (without noise) and it was robust to the errors added on measurement data. Most of the noise measurement affected the estimation of the efficiency. Despite that, the efficiency was correctly estimated.

The inverse problem established in this communication was applied to a heat conduction problem. As said in the first chapters of this communication, the convective transport during welding is not negligible. As a consequence, this inverse heat transfer problem will consider soon the convective transport in order to give interesting and reliable results.

References:

- [1] H.G. Fan, H.L. Tsai, S.J. Na. *Heat transfer and fluid flow in a partially or fully penetrated weld pool in gas tungsten arc welding*, International Journal of Heat and Mass Transfer 44 (2001) 417-428.
- [2] Traidia A., F. Roger, A. Chidley, J. Schroeder, T. Marlaud. *Effect of Helium-Argon Mixtures on the Heat Transfer and Fluid Flow in Gas Tungsten Arc Welding*, World Academy of Science, Engineering and Technology 73 (2011).
- [3] W. Zhang, J.W. Elmer, T. DebRoy. *Modeling and real time mapping of phases during GTA welding of 1005 steel*, Materials Science and Engineering A333 (2002) 320–335.
- [4] P-H Chang, T-L Teng. *Numerical and experimental investigations on the residual stresses of the butt-welded joints*, Computational Materials Science 29 (2004) 511–522.
- [5] A. Traidia, F. Roger, E. Guyot. *Optimal parameters for pulsed gas tungsten arc welding in partially and fully penetrated weld pools*, International Journal of Thermal Sciences 49 (2010) 1197-1208.
- [6] Kenneth C. Mills, *recommended thermo-physical values for commercial alloys*, Woodhead publishing limited (2002).
- [7] S. Unnikrishnakurup, S. Rouquette, F. Soulié, G. Fras. *Multiphysic modelling of GTAW Process and experimental validation for investigating weld pool behaviour*, Proceedings of the 10th International Seminar Numerical Analysis of Weldability, Schloss Seggau, Austria (2012).
- [8] A.N. Tikhonov, V.Y. Arsenin, *Solutions of Ill-Posed Problems*, Winston, Washington, DC, 1977
- [9] D.A. Murio, *The Mollification Method and the Numerical Solution of Ill-Posed Problems*, Wiley, New York, 1993.
- [10] O.M. Alifanov, E.A. Artyukhin, S.V. Rumyantsev. *Extreme Methods for Solving Ill-Posed Problems with Applications to Inverse Heat Transfer Problems*, Begell House, New York, 1995.
- [11] Y. Jarny, M.N. Ozisik, J.P. Bardon. *A general optimization method using adjoint equation for solving multidimensional inverse heat conduction*, Int. J. Heat Mass Transfer 34 (11) (1991) 2911-2919.
- [12] M. N. Necati and H. R. Orlande. *Inverse heat transfer, fundamentals and applications*. Taylor and Francis, New York (2000).